EFFECT OF THE Ni^{2+}ION BINDING ON THE STABILITY AND CONFORMATION OF BSA MOLECULE

MARINELA DIEACONU, ANA IOANID[*], STEFAN ANTOHE
Faculty of Physics, University of Bucharest

Insertion by binding of the nickel into the active sites of any representative proteins generates the biological systems as nickel-processing systems, with molecular recognition, nickel transport and enzymatic functions. In this paper we present UV-absorbance spectra of the Ni^{2+}-binding BSA recorded for $[Ni^{2+}] \in [0.01 \div 1.00] \times 10^{-4} M$ in solutions with the 1:1 stoichiometry of the $BSA : Ni^{2+}$ system and also SEM images of both the free and Ni^{2+}-complexed BSA layers deposited on a porous silicon (PS) substrate and propose an analysis of both the binding process and effect of the $[Ni^{2+}]$ on the stability and conformation of BSA molecule. The results tend towards the BSA utility as biosensor component of biodevices, such as active layer deposited on a PS substrate as transducer.

1. Introduction

Serum albumin is the most abundant protein in blood plasma and most commonly studied are human serum albumin (HAS), bovine serum albumin (BSA), equine serum albumin (ESA) and rat serum albumin (RAS), but for experiments BSA is available at high purity and low cost. Serum albumin is a very flexible protein that changes molecule shape with variations in environmental conditions and with binding of ligands.

Studies of the optical absorption properties are the redoubtable tools to understanding the electronic properties of the proteins. The changes in observed absorption spectra are correlated to conformation of the molecular geometry for any given conditions, as binding anions/cations ligands, environment, solvent, temperature.

In vivo, the tertiary structure defines the overall shape of a single protein molecule and controls the basic function of the protein. Generally this structure consists into an hydrophobic core with the terminals often charged, with a spatial configuration stabilized by the hydrogen bonds, disulphide bonds, salt bridges or posttranslational modifications.

Molecules in proteins have a complex structure, and their fundamental properties although partial unknown are exploited in novel electronic and optoelectronic molecular devices.

Electronic properties of the protein determine its functions in biological systems, so their knowledge may be the key to a large area of future nanotechnology applications in diagnose, treatment and therapeutic drug design/release fields [1]. It is known that the transition metals catalyze various biological processes and their reactivity depends on the nature of the ligands, coordination symmetry and oxidation state of the metal. Proteins as parts of the biological systems, bind the metal ions and form new ion-protein complexes with side-chain groups as ligands.

Serum albumins (HSA and BSA) have a variety of binding sites for transition metal ions, as Cu^{2+}, Ni^{2+}, Co^{2+}, Cd^{2+}, Al^{3+} [2,3]. Insertion by binding of the nickel into the active sites of any

---

[*] Corresponding author: ana_ioanid@yahoo.com

representative proteins generates the biological systems as nickel-processing systems, with molecular recognition, nickel transport and enzymatic functions.

In vitro studies have shown that the properties of the nickel-binding proteins are strongly dependent on the metal concentration. The NMR results demonstrate that the probability that Ni^{2+} binds at N-terminal sites both of HSA and BSA, have a maximum value for Ni^{2+}/albumin molar ratio ~0.8 for HSA, and ~1 for BSA [2]. Few early studies show that the binding of Ni^{2+} to HSA and BSA is a positive cooperative process and the Hill coefficient (as cooperatively index) is strongly dependent on the ion concentration $[Ni^{2+}]$ having a maximum at $[Ni^{2+}] \sim 5.00 \times 10^{-5} M$ [4]. In this paper we present UV-absorbance spectra of the Ni^{2+}-binding BSA recorded for $[Ni^{2+}] \in [0.01 \div 1.00] \times 10^{-4} M$ in solutions with the 1:1 stoichiometry of the $BSA : Ni^{2+}$ system and also SEM images of both the free and Ni^{2+}-complexed BSA layers deposited on a porous silicon (PS) substrate and propose an analysis of both the binding process and effect of the $[Ni^{2+}]$ on the stability and conformation of BSA molecule.

2. Equilibrium constant of the binding process

2.1. The relationship between the kinetics of formation and thermodynamic properties of protein-ligand complex

Kinetics is a generic term used to describe both the rates at which processes occurs and the field associated with the study of rates. Binding and dissociation processes will be characterized not only by the equilibrium constants, but also by how fast association/dissociation occur. Equilibrium equation of the process for simple case of 1:1 stoichiometry of the reversible binding ligand L to protein R as receptor, is
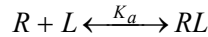
$$R + L \xleftarrow{\quad K_a \quad} RL$$

The equilibrium constant for the association process of R and L, that results in the formation of complexes RL, K_a is defined by

$$K_a = \frac{[RL]}{[R] \cdot [L]}$$

and the equilibrium constant for the dissociation process of RL complexes in R and L, K_d is defined by

$$K_d = \frac{1}{K_a} = \frac{[R] \cdot [L]}{[RL]}$$

Where $[RL]$ is the concentration of formed complexes and $[R]$, $[L]$ are the concentration of free protein and ligand, respectively, remaining in solution after complexation, at equilibrium.
Binding of ligands induces conformational transition of protein, than may be associated to a controlled functional unfolding process by a native-denatured (N-D) transition, so that to complete their benefits, these studies require multidisciplinary contributions.
If the unfolding transition N-D is reversible, so that it has become customary to view each point of transition as an equilibrium position of the interconvertible native N, and denatured D forms, respectively, and to define an equilibrium constant $K_d = K_{N-D} = \frac{[D]}{[N]}$; $[D]$ and $[N]$ being the protein concentration in denatured and native form, respectively. This constant can then be used to compute a standard free energy of the unfolding process, $\Delta G_{D-N}^0 = \Delta G^0$ [5] . Thus, using relationship between the thermodynamics and the kinetics of binding, one may write:
$$\Delta G^0 = -k_B T \ln K_d = k_B T \ln K_a$$

Experimental results show that the K_a of BSA is extremely sensitive to the concentration of high affinity ligands in the aqueous solvent. Thus, an increase in urea concentration of less than

2-fold (from 3.5 to 6 M) changes K_a by more than 100-fold. This behaviour contrasts with those of other common organic solutes, as glycine and β-alanine, that although increase the dielectric constant of solution, stabilize the native conformation of the protein rather than facilitate denaturation [6]. Biological molecules like BSA are receptors with multiple binding sites for a ligand that are initially equivalent. However, when a ligand bind to one site it induces any changes in the receptor (typically a conformational geometry change) that affect the affinity of the remaining sites for the ligand to either increase (positive cooperatively then changes in conformational flexibility are favourable for binding) or decrease (negative cooperativity then the same change are unfavourable for binding or then first binding induces any loss of freedom for entire molecule). Binding of a second molecule of the same ligand may induce yet another perturbation and so forth [7].

2.2. Binding dependence on the ligand concentration

Spectroscopic methods used for the studies of the binding/dissociation processes born out from the general feature that, when a complex is formed, the spectroscopic properties of the molecule as part of the complex may be very different than when free, both for receptor and ligand. Thus, the changes in spectroscopic signals can be used to determine the relative concentrations of free and bound ligand and/or receptor.

UV-absorbance spectroscopy is adequate because the binding/dissociation ligand-protein processes are slow on the spectroscopic time scale. The signal of the difference absorbance spectra is a mixture of complexed and uncomplexed (free) ligand, because the receptor is spectroscopically silent by compensation.

Binding energy of the ligand-protein complex that measures the affinity of partners, can be dissected into two components, namely enthalpy and entropy. At a simplistic level, enthalpy binding comes via specific (polar) molecular interactions, such as hydrogen bonds, sulphide bonds, electrostatic, van der Waals, while entropic binding results from nonspecific (apolar) hydrophobic interactions. Association kinetics of the ligand-protein complexes determines ultimately the time scale to maintain a functioning conformational state of protein.

The values of the binding constant K_a of the $BSA : Ni^{2+}$ complex may be obtained assuming the equilibrium equation of the interaction between the Ni^{2+} ion as ligand and the protein BSA as receptor, in a aqueous solution,

$$BSA + Ni^{2+} \xrightarrow{K_{ech}} BSA : Ni^{2+}$$
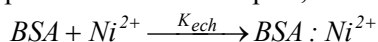
where, the equilibrium constant K_{ech} is the binding constant K_a and have equation:

$$K_a = \frac{[BSA:Ni^{2+}]}{[BSA][Ni^{2+}]}$$

In this equation, $[BSA : Ni^{2+}]$ is the concentration of the $BSA : Ni^{2+}$ complexes, $[BSA]$ and $[Ni^{2+}]$ are the concentrations of the BSA and of the free Ni^{2+} respectively, both after ligand-protein association.

Assuming $[BSA : Ni^{2+}] = c_B$ as $BSA : Ni^{2+}$ complexes molar concentration, equal with the binding sites molar concentration on BSA molecule, c_{BSA} and $c_{Ni^{2+}}$ as the analytical molar concentration of BSA and Ni^{2+} respectively, in solution, we have

$$K_a = \frac{c_B}{(c_{BSA} - c_B)(c_{Ni^{2+}} - c_B)}$$

According to Beer-Lambert law, the initial free BSA and complexed $BSA : Ni^{2+}$ solution molar concentration are given by

$$c_{BSA} = \frac{A_0}{\varepsilon_{BSA}\ell}$$

$$c_B = \frac{A - A_0}{\varepsilon_B \ell}$$

Where A_0 and $A - A_0$ are absorbance of free BSA and Ni^{2+} binding BSA solution from that have been substracted the free BSA contribution, respectively, ε_{BSA} and ε_B are the molar extinction coefficient of free BSA and Ni^{2+}-binding BSA, respectively, and ℓ is width of the cuvette.

For weak binding affinities and considering that the active (binding) sites of BSA molecule is low, then $c_B << c_{Ni^{2+}}$ and processing the equation of κ_a one obtain the equation:

$$\frac{A_0}{A - A_0} = \frac{\varepsilon_{BSA}}{\varepsilon_B} + \frac{\varepsilon_{BSA}}{\varepsilon_B}\frac{1}{K_a}\frac{1}{c_{Ni^{2+}}}$$

At saturation limit $(t \to \infty), A - A_0 \to A_\infty - A_0$ and the equilibrium condition may be transposed for the absorbance data using the reciprocal plots based to following equation:

$$\frac{1}{A - A_0} = \frac{1}{A_\infty - A_0} + \frac{1}{(A_\infty - A_0)}\frac{1}{K_a}\frac{1}{c_{Ni^{2+}}}$$

The double reciprocal plot of $\left(\frac{1}{A - A_0}\right)_\lambda$ versus $\frac{1}{c_{Ni^{2+}}}$ fits a linear dependence and the binding constant κ_a may be estimated from the ratio of the intercept at the slope a given foton energy [8].

3. Experimental results

3.1. Samples and method

We present an analysis of the UV-absorbance spectra of the $[BSA:Ni^{2+}]:[1:1]M$ system in phosphate buffer solution for $(200 \div 350)nm$ spectral range. A set of spectra were recorded as a single spectrum for each of eight values of the analytical concentration $c_{Ni^{2+}} \in [0.01 \div 1.00] \times 10^{-4} M$ in solution, Fig.1.
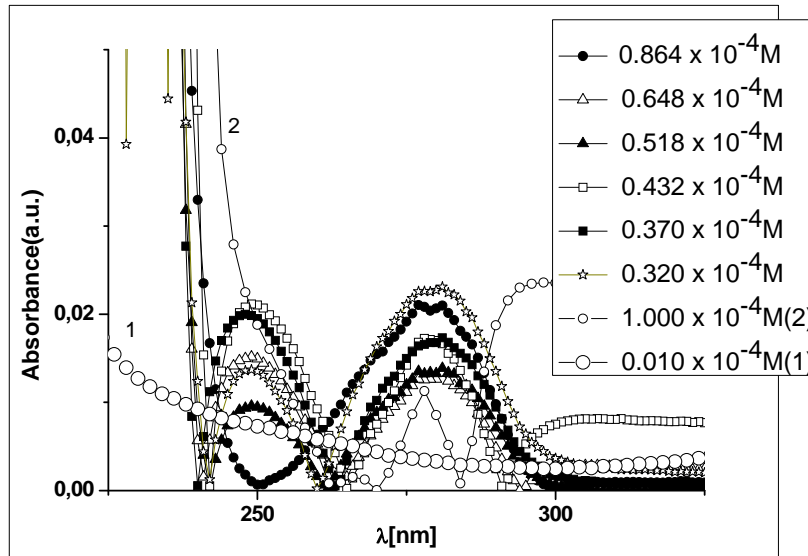

Fig.1. Difference absorbance spectra of the $[BSA:Ni^{2+}]:[1:1]M$ system:
$(-\circ)\, c_{Ni^{2+}} = 0.01 \times 10^{-4} M$; $(-\circ-)\, c_{Ni^{2+}} = 1.00 \times 10^{-4} M$;

$$(-\bullet-)\ c_{Ni^{2+}} = 0.864 \times 10^{-4}\,M\ ;\ (-\Delta-)\ c_{Ni^{2+}} = 0.648 \times 10^{-4}\,M\ ;$$

$$(-\blacktriangle-)\ c_{Ni^{2+}} = 0.518 \times 10^{-4}\,M\ ;\ (-\square-)\ c_{Ni^{2+}} = 0.432 \times 10^{-4}\,M\ ;$$

$$(-\blacksquare-)\ c_{Ni^{2+}} = 0.37 \times 10^{-4}\,M\ ;\ (-\ast-)\ c_{Ni^{2+}} = 0.32 \times 10^{-4}\,M$$

BSA with electrophoretic purity were purchased from Sigma Laboratories and nickel chlorate p.a. (NiCl$_2$) from Reactivul Laboratories, Romania were used as the source of the Ni^{2+} in solution.

All samples were prepared with the phosphate buffer solutions containing 8 g NaCl, 0.2g KCl, 1.44 g Na$_2$HPO$_4$,0.24g KH$_2$PO$_4$ and distilled water for $1000cm^3$ solution. The pH-value has been adjusted to

$(7 \div 7.4)$ with NaOH 0.1M solution. BSA (66.430 mg) and NiCl$_2$ (0.130 mg) was been dissolved in $10cm^3$ of phosphate buffer solution for $1.00 \times 10^{-4}\,M\,[\,BSA : Ni^{2+}\,][\,1:1\,]M$ sample. Solutions with any decreasing concentration were obtained by the controllable successive dilution.

We present also any SEM images of both the free *BSA* and Ni^{2+} - *BSA* complexed *BSA* layer deposited on a PS substrate from the same solution, Fig.2.
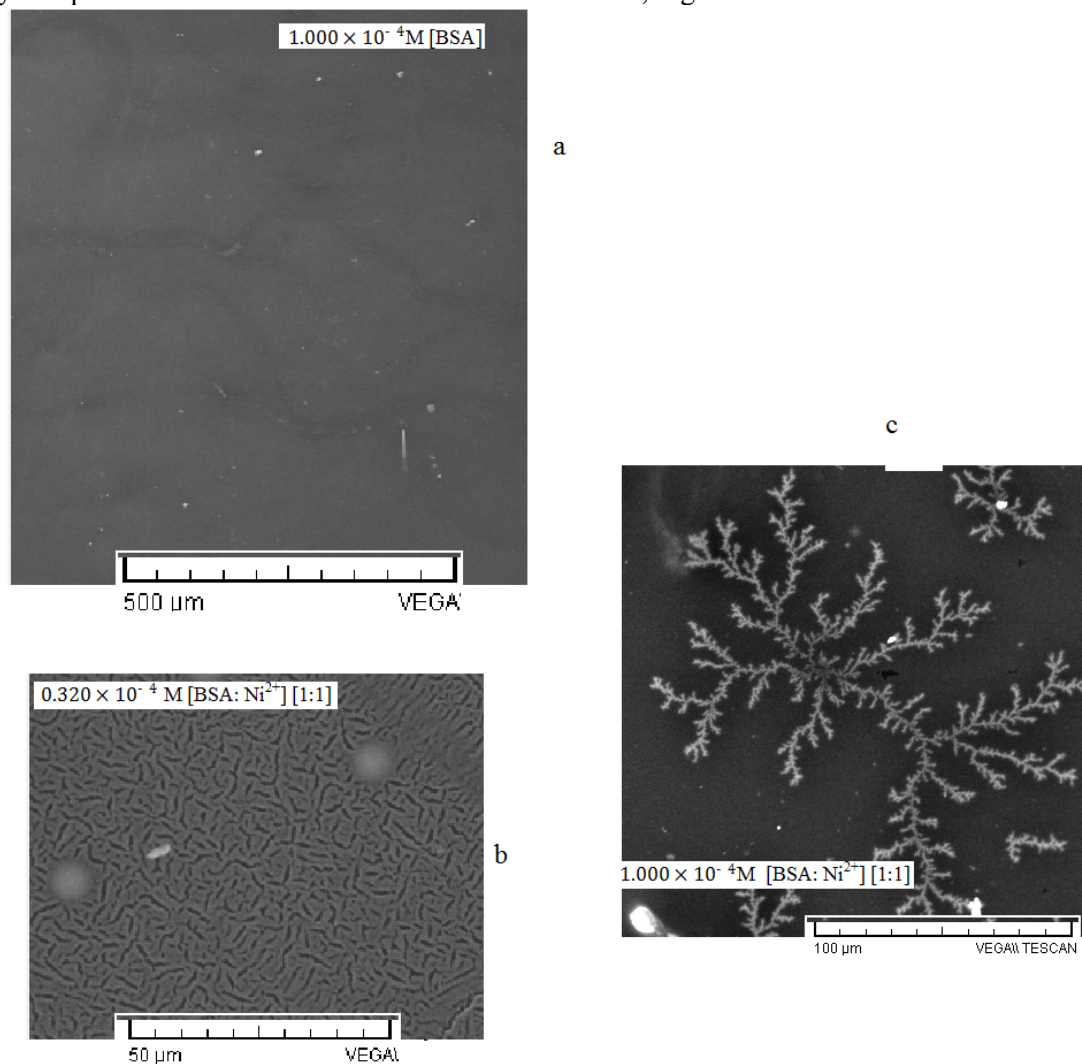

Fig. 2. SEM images for systems: a) BSA layer deposited from solution $1.00 \times 10^{-4}\,M$
[BSA]; b)BSA layer deposited from solution $0.32 \times 10^{-4}\,M\,[\,BSA : Ni^{2+}\,][\,1:1\,]M$; c)
BSA layer deposited from solution $1.00 \times 10^{-4}\,M\,[\,BSA : Ni^{2+}\,][\,1:1\,]M$

The PS substrate were formed by the etching process of a <100> p-type single crystal wafer of resistivity $\rho \sim (1 \div 3)\Omega cm$. The typical area of the sample is $\sim 1.5cm^2$. In order to provide a uniform current distribution across the surface, an aluminium layer was deposited on the back side of sample. A platinum wire netting has been used as cathode of the cell. The cell were immersed into HF and ethanol solution taken in volume ratio 1:3. The sample were obtained using a AMMT GmbH set-up under 20 mA/cm² current density in 600 s anodisation time. In order to prevent a later oxidation process in air, the sample were lateral anodized into a propylene cell using any usual technical values of the anodisation current. Protein layers were deposited from the solution that were placed on surface of the fresh PS sample for 3 h in air, then removing the solution excess.

All the difference absorbance spectra between $[BSA:Ni^{2+}][1:1]M$ sample cell and BSA reference cell, were recorded using a Perkin Elmer Lambda 35 Spectrofotometer in $(190 \div 1100)nm$ spectral range, at room temperature under ambient conditions.

SEM images of both free BSA and complexed $BSA:Ni^{2+}$ layers on PS substrate were recording with a TESCAN VEGA XM microscope.

3.2. UV-absorbance spectra depending on the $[Ni^{2+}]$

The changes of spectrum of the $[BSA:Ni^{2+}][1:1]M$ system are strongly dependent on the binding ion concentration, $[Ni^{2+}]$. The Fig.1 shows the difference absorbance spectra of the $c_x[BSA:Ni^{2+}][1:1]M$ systems, with $x \in (0.01 \div 1.00) \times 10^{-4}M$, each recorded as the first spectrum.

Mains features of spectra: i) the absorbance spectrum structure is not different on background for the $c_{BSA} = c_{Ni^{2+}} \sim 10^{-6}M$ that is far on the physiological value of $c_{BSA} \sim 10^{-4}M$; ii) for $c_{BSA} = c_{Ni^{2+}} = 1 \times 10^{-4}M$, the spectrum shows an relative intens peak at $\lambda = 280nm$, a weak peak at $\lambda \approx 266nm$ and an increasing with a should, slightly above $\lambda = 250nm$; iii) then $c_{BSA} = c_{Ni^{2+}}$ decreases, the peak at $\lambda = 280nm$ becomes large and has a structure that include the peak $\lambda \approx 266nm$, and a new distinct peak appears at $\lambda = 250nm$; iv) the height of all the peaks have a dependence with maximum and minimum on the $[Ni^{2+}]$; v) then $c_{BSA} = c_{Ni^{2+}}$ decreases, while the absorbance A_{280} decreases, the absorbance A_{250} increases; the trend of the dependence on the $[Ni^{2+}]$ for A_{280} and A_{266} is opposed to those of A_{250} in the considered spectral range, Fig.3.
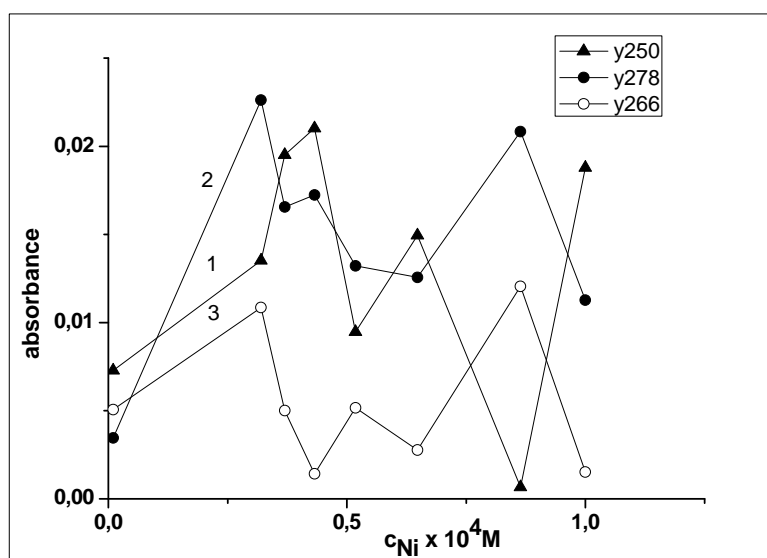
Fig.3. Dependence of the A_{280}, A_{266}, A_{250} absorbances on the $[Ni^{2+}]$

Using $A_{280} = A - A_0$ from Fig.3, we obtain from the double reciprocal plot of $\left(\dfrac{1}{A - A_0}\right)_{280}$ versus $\dfrac{1}{c_{Ni^{2+}}}$ the equilibrium constant of the association reaction, K_a, Fig.4. K_a is the ratio of the intercept and slope, has dimensions mol^{-1}, and value per molecule is $\dfrac{K_a}{N_A}$, where N_A is Avogadro's number.
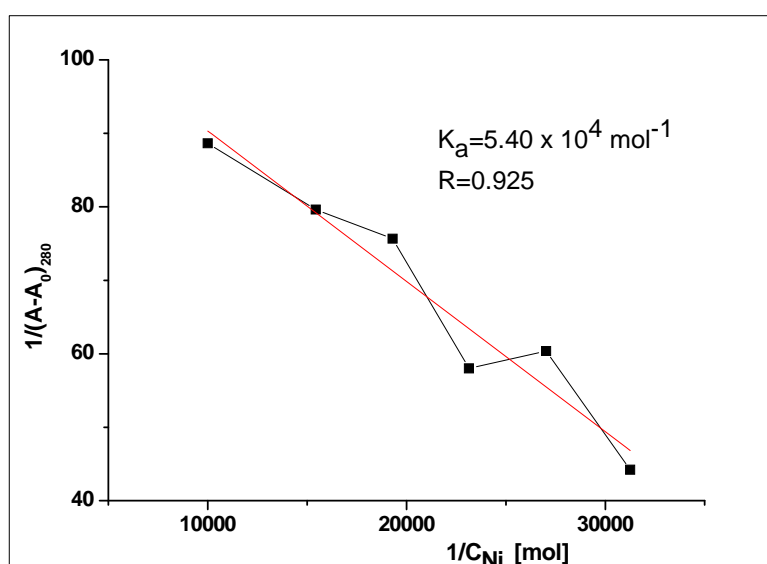

Fig.4. Double reciprocal plot $\left(\dfrac{1}{A - A_0}\right)_{280}$ versus $\dfrac{1}{c_{Ni^{2+}}}$ using $A_{280} = A - A_0$ for determination of the equilibrium (binding) constant (it has been used only decreasing portion).

3.3. SEM images of the free BSA and $BSA:Ni^{2+}$ layers on PS substrate

SEM images from Fig.2 show a strongly different surface morphology between the free BSA and complexed $BSA:Ni^{2+}$ layers deposited on PS substrat . Thus, while the free BSA layer shows any large compact regions (a), the complexed $BSA:Ni^{2+}$ layer shows a dendritic structure (b) and (c) whose the compactity depends on the $[Ni^{2+}]$ in solution of deposition.Thus, for low $[Ni^{2+}]$ values of $0.32 \times 10^{-4} M [BSA:Ni^{2+}][1:1]M$, the complexed $BSA:Ni^{2+}$ layer has a greater density of small dendrites (b), while for large $[Ni^{2+}]$ values of $1.00 \times 10^{-4} M [BSA:Ni^{2+}][1:1]M$ the thinned layer consists into greater dendrites (c). Taking into account that the structure morphology depends on the interactions between BSA and PS, it is resonable to consider that the adhesion interactions are different corresponding to any different exposures of the BSA molecule.

The free BSA layer is obtained by the adsorption of the almost globular molecules of the free (native) BSA, while the complexed $BSA:Ni^{2+}$ layer is obtained by adsorption of a deformated molecule of the Ni^{2+}-binding BSA. The complexed $BSA:Ni^{2+}$ layer shows a dendritic structure whose the compactity depends on the $[Ni^{2+}]$ in solution of deposition.Thus, for low $[Ni^{2+}]$ values, the complexed $BSA:Ni^{2+}$ layer has a greater density of small dendrites (b), while for large $[Ni^{2+}]$ values the thinned layer consists into greater dendrites (c). Deformation degree and consequently the exposure of the Ni^{2+}-binding BSA molecule to PS surface depend on the $[Ni^{2+}]$ value in solution. This results supports the above considerations about the dependence of the Ni^{2+} affinity at the binding sites of BSA on the $[Ni^{2+}]$ and agree with the the absorbance dependence on the $[Ni^{2+}]$ value in solution (Fig.1). At low $[Ni^{2+}]$ values , the affinity of Ni^{2+} is greater for bonding sites of BSA from any smaller loops that being less numerous induce only reduced deformations. On the contrary, at high $[Ni^{2+}]$ values, the high afiinity for bonding sites from numerous greater loops induce a significante deformation of BSA molecule.

4. Discussions

4.1. Dependence of the UV absorption spectrum on the $[Ni^{2+}]$

Structure of the proteins absorbance spectrum in the near-UV range, between $\lambda = 240nm$ and $\lambda = 300nm$ is associated to the transitions of the delocalised electrons of the side-chain aromatic residues tryptophan (Trp), tyrosine (Tyr), cysteins (Cys) bonded by disulphide bonds (S-S) and phenylalanine (Phe), while in the far-UV range, between $\lambda = 180nm$ and $\lambda = 240nm$, to the electronic transitions HOMO-LUMO orbital states of the amide groups of the all main-chain-side residues [9].

Peak of the absorbance at $\lambda \in (275 \div 280)nm$, for more proteins and particulary for free $[BSA] \sim 10^{-4} M$ in solution, is due to the absorbance of the Trp, Tyr and Cys S-S bonds, so that the molar extinction coefficient may be expressed as $\varepsilon_{280} = \varepsilon_{Trp} \cdot n_{Trp} + \varepsilon_{Tyr} \cdot n_{Tyr} + \varepsilon_{SS} \cdot n_{SS}$. In folded (native, functional) conformation, BSA standard has $n_{Trp} = 3, n_{Tyr} = 21, n_{SS} = 34$ [10]. The absorbance of Trp and Tyr residue depends on the polar/nonpolar environment of their chromophores, so that for the native conformation in solution, the residues exposed to solvent and those from inside of protein will absorb differently. As consequence of a change of the protein conformation, the ratio of exposed to solvent/inside protein residues is changed also. Thus, the

absorbance spectrum is very sensitive to the conformational change of protein, for example by ligand-binding protein interactions.

Peak of the absorbance at $\lambda \approx 260nm$ for free BSA in solution has two contributions: one of the Phe residues whose absorption determines the fine structure of spectrum in $\lambda \in (250 \div 260)nm$ range, and other of the near UV-band at $\lambda \approx 260nm$ of the S-S bonds between Cys pairs. [11]. In the native state, the BSA molecule has 17 S-S bonds between pairs of Cys groups on side-chain sites and a Cys side-chain site free. These bonds delimit 9 fragments (loops) organized in 3 domains that constitute the tertiary structure in the native form of the protein at neutral pH and normal temperature[12]. Disulphide bond S-S between the thiol (-SH) groups of the two adjacent Cys residues is a strong covalent bond, so that the binding energy of the electron in HOMO orbital states of the group in Cys is greatly diminished. Accordingly, present or broken any intramolecular S-S bonds can induce changes in the HOMO-LUMO orbital states gap measured by the optical absorption in the electronic transitions [13].

Partial breaking of the S-S bond system changes the macromolecule shape so that the fragments delimited by these bonds have a greater exposure to solvent. Exchange reaction S-S bonds/(-SH) free groups and other non-covalent interactions, may occur sequentially, with rates that depend on the characteristics of the solution, pH, ionic strength, temperature [1].

Breaking of S-S bonds by binding via the protein complexation process with transition metal ions is one way of denaturation of the protein by favouring a specific molecular conformation.[14,15].

It is known that the Ni^{2+} ion forms complexes with a planar geometry having four N-terminal atoms as ligands, from that one is a δN-terminal atom of the imidazole group of the His residue. [16].

Protein fragments delimited by the S-S bonds have both the composition and length different, so that the His residues have any different neighborhood, mainly dominated by hydrophobic groups that will be exposed to solvent by the protein denaturation.

Preference of the metal ion to coordinate with His groups from different fragments of the protein, depends on its nature, and for a given ion depends on the pH of the solution and on the neighborhood with hidrophobe groups of binding position. Thus, for BSA having the His[111] and His[96] groups in fragments with the different lengths, while the Cu^{2+} ion affinity is higher for His[96] (situated in a longer fragment) than for His[111] (situated in a shorter fragment), the Ni^{2+} ion has higher affinity for His[111] than for His[96]. [17]. Thus, the Ni^{2+} ion binding can induces the breakage of the S-S bonds that close the smaller fragments.

Changes in the absorbance spectrum of the proteins in the far UV-range are associated to the changes of the electronic states distribution of the whole molecule. Thus, the changes of the UV spectrum of the complexed $BSA : Ni^{2+}$ system comparative to the free BSA, show the conformational changes of the BSA molecule induced by the metal ion binding.

Binding of the Ni^{2+} ion to the BSA molecule changes only the relative intensity of the absorbance peak A_{280} but not his spectral positions, while for $\lambda < 250nm$ spectral range, appear new absorbance peaks associated to any ligand-to metal charge transfer electronic transitions $d \rightarrow \pi^*$ to excited state of the $[BSA : Ni^{2+}][1:1]M$ complexes. [9,18,19]. Taking into account the S-S bonds röle, the changes in the UV spectrum depending on the $[Ni^{2+}]$ might be attributed to any different denaturing degrees induced by the BSA complexation; the initial binding of a number of ions to the molecule protein sites favourised by its native conformation, induces the denaturation of the molecule by the local deformation and breaking of S-S bonds; the new exposure to solvent of the BSA molecule by the fragments of different length changes both the intrinsic chromophores (associated with Trp, Tyr, Phe residues) coordination and the binding process rate because the Ni^{2+} ion has the specific affinity for the binding sites placed on the different fragments [20].

Another considerations derive from the experimental data which highlight a selective dissociation pathways for the fragments linked by the S-S bonds. Cleavage (broken) of the S-S

bonds is selectively because of their different binding energy, namely an energy of $\sim(40 \div 70)kcal/mol$ for the binding between the (-SH) groups and an energy of $\sim(25 \div 40)kcal/mol$ for the S-C binding directly linked on amide groups [21]. Increasing the intensity of the absorbance A_{250} and the symmetrical decreasing of the absorbance A_{280} with decreasing of the $[Ni^{2+}]$ in solution, shows that at low ion concentrations priority broken the S-S bonds that close the short S-S loops on whose fragments the binding takes place at sites with higher affinity.

4.2. Morphology of the free BSA and $BSA:Ni^{2+}$ layers on PS substrate

As is known, BSA and also other proteins or macromolecular organic compounds, is biosensor component of many types of biodevices, such as active layer deposited on a PS substrate as transducer [22,23].

Biosensor efficiency measured by the amplitude change of physical properties of the transducer (PS substrat) depends on the type and strength of the adhesion interactions of BSA layer at the PS surface. On the other hand, the specific or non specific interactions between BSA and PS depend on both the nature of the PS surface, hydrophilic or hydrophobic, and orientation of the BSA molecule which tends to exhibit terminals to interact attractive with PS. As a consequence, layer deposited from free BSA solution with almost globular molecule will have different morphology from that of the $BSA:Ni^{2+}$ system layer, with deformated to an elongated molecule of same deposition conditions.

The complexed $BSA:Ni^{2+}$ layer shows a dendritic structure whose the compactity depends on the $[Ni^{2+}]]$ in solution of deposition.Thus, for low $[Ni^{2+}]$ values, the complexed $BSA:Ni^{2+}$ layer has a greater density of small dendrites (b), while for large $[Ni^{2+}]$ values the thinned layer consists into greater dendrites (c). Deformation degree and consequently the exposure of the Ni^{2+}-binding BSA molecule to PS surface depend on the $[Ni^{2+}]$ value in solution. This results supports the above considerations about the dependence of the Ni^{2+} affinity at the binding sites of BSA on the $[Ni^{2+}]$ and agree with the the absorbance dependence on the $[Ni^{2+}]$ value in solution (Fig.1). At low $[Ni^{2+}]$ values , the affinity of Ni^{2+} is greater for bonding sites of BSA from any smaller S-S loops that being less numerous induce only reduced deformations of the BSA molecule. On the contrary, at high $[Ni^{2+}]$ values, altough the Ni^{2+} afiinity for bonding sites from numerous greater S-S loops is low and the number of the $BSA:Ni^{2+}$ complexes is low also, the breaking of greater S-S bonds induce a significante deformation of BSA molecule.

Thus, the significant changes of the SEM image aspect of the free BSA layer compared to those of the $BSA:Ni^{2+}$ system layer can be associated with any significant conformational changes of the BSA molecule by binding of Ni^{2+} ions, and these changes depend on the $[Ni^{2+}]$ in solution of deposition.

5. Conclusions

The changes of spectrum of the $[BSA:Ni^{2+}][1:1]M$ system are strongly dependent on the $[Ni^{2+}]$. For $c_{BSA}=c_{Ni^{2+}}=1\times10^{-4}M$, the spectrum shows an relative intens peak at $\lambda=280nm$, a weak peak at $\lambda\approx266nm$ and an increasing with a should, slightly above $\lambda=250nm$; iii) then $c_{BSA}=c_{Ni^{2+}}$ decreases, the peak at $\lambda=280nm$ becomes large and has a

structure that include the peak $\lambda \approx 266\,nm$, and a new distinct peak appears at $\lambda = 250\,nm$; while the absorbance A_{280} decreases, the absorbance A_{250} increases. Binding of the Ni^{2+} ion at BSA molecule induces any conformational changes that give to any morphological changes of the complexed $BSA:Ni^{2+}$ layer deposited on a PS substrate. While the free BSA layer is almost compact, the complexed $BSA:Ni^{2+}$ layers show a dendritic structure whose the compactity depends on the $[\,Ni^{2+}\,]$ in solution of deposition.

Because it is plausible to consider that the deformation of the almost globular native BSA molecule to one elongated by the complexation with Ni^{2+} may be attributed to the breaking of any S-S bonds, the morphologies of the complexed $BSA:Ni^{2+}$ layers show that the cleavage of S-S bond system enhances with the increasing of the $[\,Ni^{2+}\,]$ in solution of deposition.

References

[1] Philippe Rondeau, Giovanna Navarra, Valeria Militello, and Emmanuel Bourdon, Protein aggregation, Chap.5, pp 1-22, ISBN 978-61761-815-4, 2010 Nova Publishers, Inc., Ed.Douglas A. Stein, email: rophil@univ-reunion.fr

[2] Peter J.sadler, Alan Tucker and John H. Viles, Eur. J. Biochem. **220**, 193 (1994).

[3] Thomas J Meade, Alisha K. Taylor and Steven R Bull, Current Opinion in Neurobiology **13,** 597 (2003).

[4] Zhou Yongoia, Hu Xuing, Ouyang Di, Huang Jiessheng and Wang yumen, Biochem. J. **304**, 23 (1994).

[5] A.Szilagyi, J.Kardos, L.Barna, P.Zavodschi, 10 Protein folding, Springer-Verlag Berlin Heidelberg 2007, pag 16

[6] Irvin M.Klotz, Proc.Natl. Acad. Sci. USA, Biochemistry **93**, 14411(1996).

[7] http://www.123people.com/s/charles+r+sanders

[8] Regis Marty, Christophe N. N'soukpoe-Kossi, David M. Charbonneau, Laurent Kreplak, Heldar-Ali Tajmir-Riahi, Nucleic Acids Research, **37**(15), 5197 (2009).

[9] M.Dieaconu, A.Ioanid, S.Iftimie, S.Antohe, Digest Journal of Nanomaterials and Biostructures, **7**(3), 1125 (2012).

[10] S.C.Gill and P.H.von Hippel, Anal.Biochem. **182**,319 (1989).

[11] Franz-Xaver Schmid, Biological Macromolecules: UV-visible Spectrophotomatry, ENCYCLOPEDIA OF LIFE SCIENCES, 2001,www.els.net

[12] P.Restani, C.Ballabio, A.Cattaneo, P.Isoardi, L. Terracciano, A. Fiocchi, Allergy **59**(Suppl.78), 21 (2004).

[13] R.Maul, M.Preuss, F. Ortmann, K. Hannewald, and F. Bechstedt, J.Phys. Chem., A, **111**, 4370 (2007).

[14] Mikel J. Lindberg, Johanna Normark, Arne Holmgren, and Mikel Oliveberg, PNAS, **101**(45), 15893 (2004).

[15] Sanja Ostojic, Vida Dragutinovic, Miodrag Kicanovic and Branislav R. Sominovic, J.Serb.Chem.Soc., **72**(4), 331 (2007).

[16] Peter J. Sadler, Alan Tucker and John H. Viles, Eur. J. Biochem. **220**,193 (1994).

[17] Mark Klewpatinond and John H. Viles, Biochem.J., **404**, 393 (2007).

[18] B.Bosnich, Contribution from the William Ramsay and Ralph Forster Laboratories, university College, London W.C.1,England, pp 627-632, 1967.

[19] E. Frason, C. Panattoni, and L.Sacconi, J.Phys. Chem., **63**, 1908 (1959).

[20] Mark Klewpatinond and John H. Viles, Biochem.J., **404**, 393 (2007).

[21] S-S_thesis, williammurad.com/docs/murad_thesis.pdf

[22] Luca De Stefano, P. Arcari, A. Lamberti, C.Sanges, L. Rotiroti, I.Rea,and I.Rendina, Sensors, **7**, 214 (2007).

[23] M.Staiano, M.de Champdoré, S. Borini, A.M. Rossi, M. Rossi and S. D'Auria, Current Chemcial Biology, **1,** 3 (2007).